LDEF MICROENVIRONMENTS, OBSERVED AND PREDICTED*

R. J. Bourassa, H. G. Pippin and J. R. Gillis
Boeing Defense and Space Group
P. O. Box 3999, M/S 82-32
Seattle, WA 98124
Phone: 206/773-8437; Fax: 206/773-4946

SUMMARY

A computer model for prediction of atomic oxygen exposure of spacecraft in low earth orbit, referred to herein as the primary atomic oxygen model, was originally described at the First LDEF Post-Retrieval Symposium (ref 1). The primary atomic oxygen model accounts for variations in orbit parameters, the condition of the atmosphere, and for the orientation of exposed surfaces relative to the direction of spacecraft motion. The use of the primary atomic oxygen model to define average atomic oxygen exposure conditions for a spacecraft is discussed herein and a second mircoenvironments computer model is described that accounts for shadowing and scattering of atomic oxygen by complex surface protrusions and indentations. Comparisons of observed and predicted erosion of FEP thermal control blankets using the models are presented. Experimental and theoretical results are in excellent agreement. Work is in progress to expand the modeling capability to include ultraviolet radiation exposure and to obtain more detailed information on reflecting and scattering characteristics of material surfaces.

INTRODUCTION

Atomic oxygen erosion of materials varies with exposure conditions and differences in the geometry of exposed surfaces. Modeling of atomic oxygen exposure is needed to derive material performance parameters from orbital test data. Modeling is also important in design of hardware to be used under conditions differing from those of test. Two computer models have been developed to define atomic oxygen exposure for a spacecraft in low earth orbit. The first of these is a primary atomic oxygen model that accounts for orbit altitude, atmospheric conditions, mission duration, surface orientation and other factors that define the macroenvironment. The primary atomic oxygen model was discussed at the First LDEF Post-Retrieval Symposium (ref 1) and is described in further detail in NASA Contractor Report 189627 (ref 2). The second model, presented herein, accounts for the effects of complex surface protrusions and indentations of spacecraft equipment on atomic oxygen exposure. These variations in geometry alter the atomic oxygen exposure environment by casting shadows, producing reflections and scattering incident atomic oxygen flux. The microenvironments model accounts for any arbitrary size, shape, orientation, or curvature of exposed surfaces and for interferences between nearby surfaces. The task of modeling atomic oxygen exposure is simplified by using the two models together. The first model is used to reduce orbital and atmospheric variables to mission average conditions. The second model is used to account for variations in detailed design of exposed hardware.

The LDEF experiment offers an ideal opportunity to compare model predictions with observations. Data are presented herein showing comparisons of predicted erosion with experimental results for FEP thermal control film at three locations on LDEF. Experimental and

* Work done under Contract NAS1-19247

theoretical erosion of surfaces shows similar trends. The magnitudes of observed and predicted erosion of FEP blankets are in agreement even for surfaces of very complex shape.

OBJECTIVE

To show how the primary atomic oxygen model may be used to define average conditions of exposure for a spacecraft over extended periods of time, to describe the microenvironments model for atomic oxygen exposure, and to verify the accuracy of both models by comparing observed and predicted atomic oxygen effects on FEP thin film materials flown on LDEF.

PRIMARY ATOMIC OXYGEN MODEL AND AVERAGE EXPOSURE CONDITIONS

The details of the primary atomic oxygen model are presented in Reference (2). A summary of the factors affecting atomic oxygen exposure handled by the model are shown in Figure 1. All of the factors shown in Figure 1 significantly affect exposure. Orbit altitude and atmospheric conditions are especially important. At an altitude of 400 km, a 25 km decrease in altitude causes atomic oxygen density to increase by 50 percent. At this same altitude, atomic oxygen densities may differ by a factor of 20 between maximum and minimum conditions of solar activity.

These wide swings in the severity of the exposure environment make it necessary to integrate atomic oxygen rates with time to determine precise exposures. It was not considered practical to add further to the complications of the calculation by linking microenvironment variables directly to the integration. The solution to this complex problem is to divide it into parts that can be handled in succession. Fluences to plane surfaces of a spacecraft can be calculated efficiently with the primary model while treating the variables shown in Figure 1. The results of the primary exposure calculation are then used to define average exposure conditions for a mission or pertinent portions of a mission. These constant average conditions for the macroenvironment become inputs for the microenvironments model.

The calculation of average conditions from fluences to plane surfaces on a vehicle is very straight forward. The required formulas are readily derived from Equation (8) presented in Reference (2). Resulting equations for the average conditions are as follows:

$$F_0 = (\text{Fluence in ram direction})/(\text{Time for event or mission}) \quad (1)$$

$$F_{90} = (\text{Fluence } 90^\circ \text{ to ram direction})/(\text{Time for event or mission}) \quad (2)$$

$$N_{Average} = F_0/(\text{Average orbital speed}) \quad (3)$$

$$\langle c \rangle = 4F_{90}/N_{Average} \quad (4)$$

$$T_{Average} = (\pi M/8R)\langle c \rangle^2 \quad (5)$$

Where:

<c>	Average molecular speed, cm/sec
F	Atomic oxygen flux, atoms/cm^2-sec
M	Molecular weight, 16.00 g/g-mole
N	Number density, molecules/cm^3
R	Universal gas constant, 8.314 x 10^7 ergs/g-mole-K°
T	Absolute temperature, K°
π	Value of pi, 3.14 . . .

Averages for atomic oxygen number density, atmospheric temperature, and orbital speed together with parameters describing the geometry and surface properties of the vehicle hardware become the inputs for the atomic oxygen microenvironments model.

MICROENVIRONMENTS MODEL

The relationships between the primary atomic oxygen model and the microenvironments model are shown in the Figure 2. The purpose of the microenvironments model is to account for local geometry variations and surface conditions affecting atomic oxygen exposure. The microenvironments model uses the average conditions derived from outputs for plane noninterfering surfaces calculated using the primary model. The new variables introduced by way of the microenvironments model are those that cause shadowing and scattering of incident atomic oxygen flux.

Examples of shadowing and scattering are shown in Figure 3. Shadowing and scattering represent interactions between exposed surfaces that affect molecular flux. Shadowing is caused by irregularities on an exposed surface or its surroundings that block out a portion of the sky as seen from specific locations on the surface. Scattering is caused by either specular or diffuse reflection of incident atomic oxygen such that reflected oxygen molecules intercept another exposed surface. These effects depend on protrusions, indentations and curvature of exposed surfaces or on interference between surfaces. Neither shadowing nor scattering can affect the flux on a surface unless other nearby surfaces can be seen from points on the given surface or unless the given surface can see itself. Thus, plane surfaces facing away from each other are not affected by shadowing or scattering. The same is true of surfaces with convex curvature. Shadowing reduces molecular flux. Scattering by either specular or diffuse reflection increases molecular flux to the receiving surface.

Figure 4 shows how the microenvironments model handles shadowing and direct exposure. Direct exposure is molecular flux that reaches a surface without first being reflected by another surface. Scattered flux is determined by a Monte Carlo technique. The microenvironments program has four major elements: (1) a geometric routine; (2) a ray tracing routine; (3) a source function; and, (4) a Monte Carlo integration routine.

The geometric routine defines the shape of exposed surfaces and their spatial relationships. The defined surfaces may be faced in any direction. Exposed areas of entirely arbitrary shape may

be simulated. Areas of complex shape are represented by assembling simple unit surfaces and shapes. Up to 100 planes, cylinders and other shapes may be handled by the geometric routine at one time.

The ray tracing routine is very similar to other routines developed for such applications as calculating view factors for radiant heat transfer, fugitive light intensities in dark rooms, and for computation of perspective views from orthographic architectural drawings. Nodes are established for the ray tracing calculation, each representing a finite area of exposed surface. Directions are assigned to a specified number of a primary rays originating from each node. Direction is defined by two angles relative to the local surface normal and the bow of the vehicle. The ray tracing routine determines if a primary ray originating from a node on a surface can see the sky. For each unblocked direction, the projected surface area represented by the node is multiplied by the source function to determine direct flux.

The source function specifies the flux per unit solid angle that originates from a given direction in the sky. The function depends on three environmental parameters: number density, atmospheric temperature and orbital speed, all three treated as constant average values. The source function has only one independent variable, angle from the ram direction. Tabular files of this function in terms of its independent variable need be calculated only once for each use of the microenvironments program. This simplification, made possible by the primary atomic oxygen program, speeds the computations.

Reflected molecular flux is handled by a Monte Carlo technique. Each time a direction from a node is identified that is unblocked by other surfaces, primary flux is calculated for that direction and the incident flux is considered to be represented by a specified number of secondary rays for the Monte Carlo computation. A weighted random choice for disposition of the flux represented by each secondary ray is assigned as follows: reaction of atomic oxygen with the surface material; recombination of monatomic oxygen to form diatomic oxygen; specular reflection; and diffuse reflection.

If the atomic oxygen represented by a secondary ray is specularly or diffusely reflected, then the ray is followed to a new impact point and the process is repeated. The directions of rays experiencing diffuse reflection are weighted according to Lambert's cosine law. If a reflected ray does not strike the vehicle, the flux represented by the ray is considered lost to space.

If surface reaction or recombination is the random disposition selected, then the selection is noted and no further consideration is given to the atomic oxygen represented by that secondary ray. Atomic oxygen undergoing reactions at this place in the computation are cataloged only to arrive at a correct answer for reflected flux reaching surrounding areas of the exposed surface. Surface erosion is calculated later based on the total atomic oxygen flux determined for each node and a reaction coefficient for the surface material.

The integration routine tabulates two items: (1) the total direct flux reaching the finite area assigned to a node from all directions that are unblocked, and (2) the total of all reflected flux striking the assigned area. The work of this routine amounts to arithmetic and bookkeeping. Once all directions from a node have been examined, the entire summation process is repeated for the next node.

The microenvironments calculation requires properties for reflectance and reactivity of exposed surface materials. The values of reflectance used in this study, shown on Table 1, are not based on actual test data. They are only estimates made to support this initial assessment of the models. Also, it should be noted that the reaction rate coefficient was considered constant, independent of incidence angle and impact velocity. If reaction rate coefficient is later shown to be

a function of other variables, then the model can be refined to account for this dependence. The value of the reaction coefficient used is based on the average of values reported by various LDEF experimenters.

Table 1. PROPERTIES OF EXPOSED MATERIALS

PROPERTY	FEP BLANKET	ALUMINUM
Specular Reflectance	49%	50%
Diffuse Reflectance	49%	46%
Recombination and Reaction	2%	4%
Reaction Coefficient	0.34E-24 cm^3/atm	Zero

OBSERVED AND PREDICTED ATOMIC OXYGEN EFFECTS

Angle Bracket, Experiment Tray F9

Figure 5 shows the locations of the three FEP film materials that were selected for comparison of observed and predicted erosion. The first of these locations was on Experiment Tray F9. This tray carried an angle bracket that was covered on both sides with an adhesively bonded FEP film. A section of the angle bracket was made available to Boeing by McDonnell Douglas for this study.

Figure 6 shows a cross-section of the angle bracket. The bracket has three flat portions, as follows: one extending outside the envelope of the experiment tray, facing the ram vector; a second in a horizontal position nearly parallel with the ram vector; and a third recessed inside the tray envelope and facing the ram vector. Normals to the first and third portions of the bracket make an angle of 8.1 degrees with the ram vector. A normal from the second surface makes an angle of 89.2 degrees with the ram vector. The shape of the bracket defines the shape of the FEP film surface. The film covered bracket was potted in plastic and polished to display the thickness of the coating. Photomicrographs of the coating were taken along the edge of the bracket at 100 magnification. A mosaic, about 17 feet in length, was prepared from the photomicrographs. Thickness of the coating and distance from the outside edge of the bracket were scaled from the mosaic.

A comparison of observed and predicted post flight thicknesses for the angle bracket FEP covering is shown in Figure 7. The cover thickness is a minimum on the recessed portion of the bracket. This is because the recessed area was subject to exposure from both primary and reflected atomic oxygen. The calculation shows that had it not been for reflected flux, the final thickness of the cover would have been the same on both areas of the bracket facing the ram vector. Minimum erosion occurred on the portion of the bracket that was nearly parallel to the ram vector (horizontal area). Note that even this area received some reflected flux. Reflected flux reaching the horizontal portion of the bracket would have originated from the recessed area.

Observed and predicted thickness are in good agreement. Some allowance must be made for accuracy in measurements of both thickness and distance along the bracket. Also, the reflected molecular flux, both specular and diffuse are based on estimated reflectances. Trends shown by observed and predicted thickness are in good agreement. The model appears to be very accurate after allowances for accuracy of physical measurements.

Figure 8 shows three calculations of total flux for the angle bracket made with widely differing molecular reflectances. The allowance for surface recombination and reaction was held constant at 2% for these calculations. The calculation shows that if all molecular reflections were specular, then the area of the angle bracket parallel to the ram vector would not have received scattered atomic oxygen. Under this condition, the recessed area of the bracket would have received maximum scattering. Had the situation been reversed, had all scattering been caused by diffuse reflectance, then the recessed area would have received a minimum of scattered atomic oxygen and the scattered flux reaching the area parallel to the ram vector would have been maximized.

Blanket Edge Attachments, Experiment Trays B7 and D11

The leading edges of the thermal control blankets on Experiment Trays B7 and D11 face the ram vector at angles such that rolled edge portion of the blanket experiences a large variation in exposure over a short distance. Also, the experiment frame shielded the blanket between the roll and blanket edge. The geometry of the blanket edge attachment is shown in Figure 9. The only difference between the locations shown for Experiment Trays B7 and D11 is the angle the trays make with the ram vector. Comparisons of observed and predicted post flight thicknesses at these points offer an excellent opportunity for verification of the atomic oxygen exposure models.

The shape of the FEP foil at the edge attachment was estimated as closely as possible by Francois Levadou of ESTEC/ESA for this study. Measurements were taken on the experiment frame and combined with Levadou's measurements to yield the geometry shown in Figure 9. Thickness of blanket film materials were made on samples supplied to Boeing by NASA. The samples were first potted and polished, then thicknesses and edge distances were obtained from photomicrographs. Prediction of post flight thicknesses for these specimens was made using the microenvironments model.

Observed and predicted results are shown in Figures 10 and 11 for the specimens exposed on Experiment Trays B7 and D11, respectively. Good agreement between experimental observations and model predictions is displayed at both locations. Observed and predicted trends in erosion with distance measured from the blanket edge are in agreement . Measured and predicted thicknesses are within the limits of experimental accuracy.

The minimum thicknesses predicted for two exposure conditions, primary flux only and primary flux plus reflected flux, are shown in Figure 10 for the Tray B7 specimen. The two curves illustrate a noteworthy point. The minimum thicknesses predicted for primary flux only and for primary flux plus reflected flux occur at different distances from the edge of the blanket. Maximum exposure does not necessarily correspond to a zero incidence angle (between the surface normal and the ram vector) when reflected flux is considered. The difference is even more evident in the data shown in Figure 11 for the Tray D11 specimen.

CONCLUSIONS

Two computer models have been developed to predict atomic oxygen exposure of spacecraft materials. These models work together. The first model functions to calculate atomic oxygen exposure to simple noninterfering surfaces of a vehicle and to reduce orbital and atmospheric variables to mission average conditions. The second model is used to account for detailed hardware design features that may cause shadowing and scattering of atomic oxygen flux. Observed erosion of FEP samples flown on LDEF and predictions made with the models are in agreement even for specimens of complex shape.

REFERENCES

1. Bourassa, R. J., Gillis, J. R., and Rousslang, K. W.: Atomic Oxygen and Ultraviolet Radiation Mission Total Exposures for LDEF Experiments. *LDEF 69 Months in Space, First Post-Retrieval Symposium,* NASA Conference Publication 3134, 1991.

2. Bourassa, R. J. and Gillis, J. R., *Atomic Oxygen Exposure of LDEF Experiment Trays*, May 1992, NASA Contractor Report 189627.

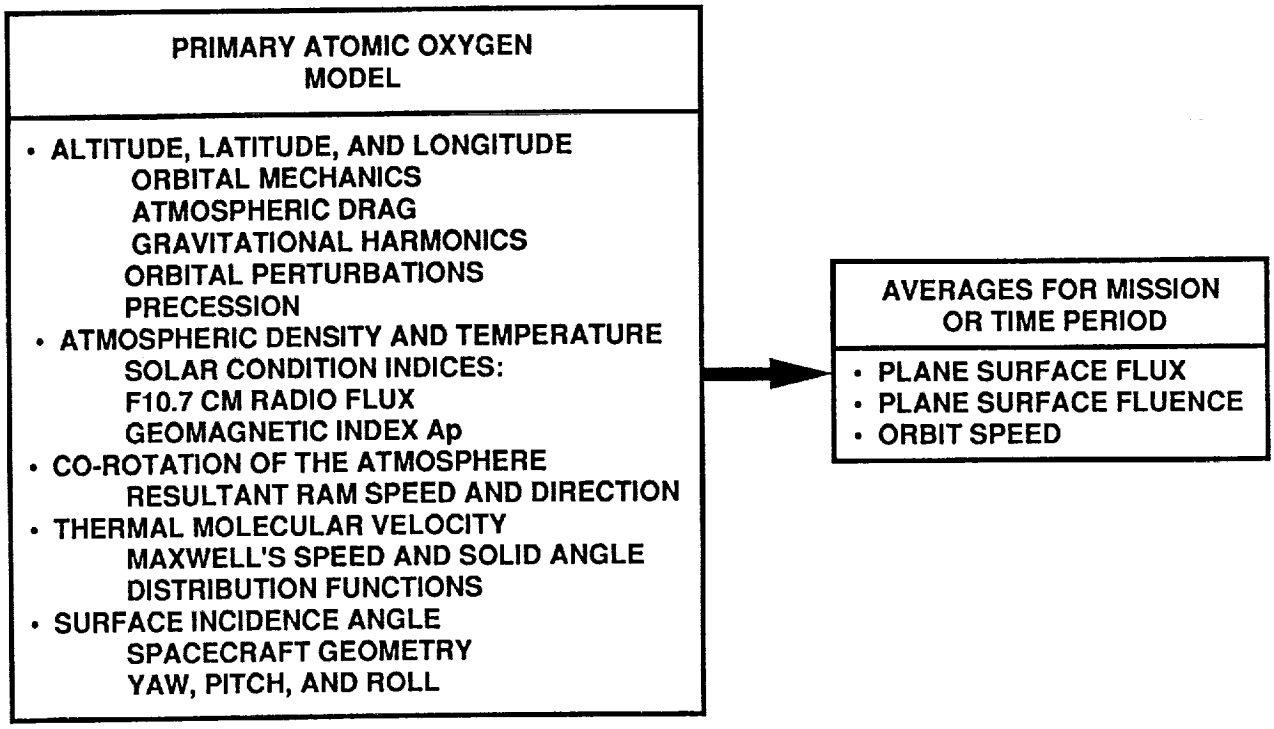

Figure 1. Attributes of the primary atomic oxygen model.

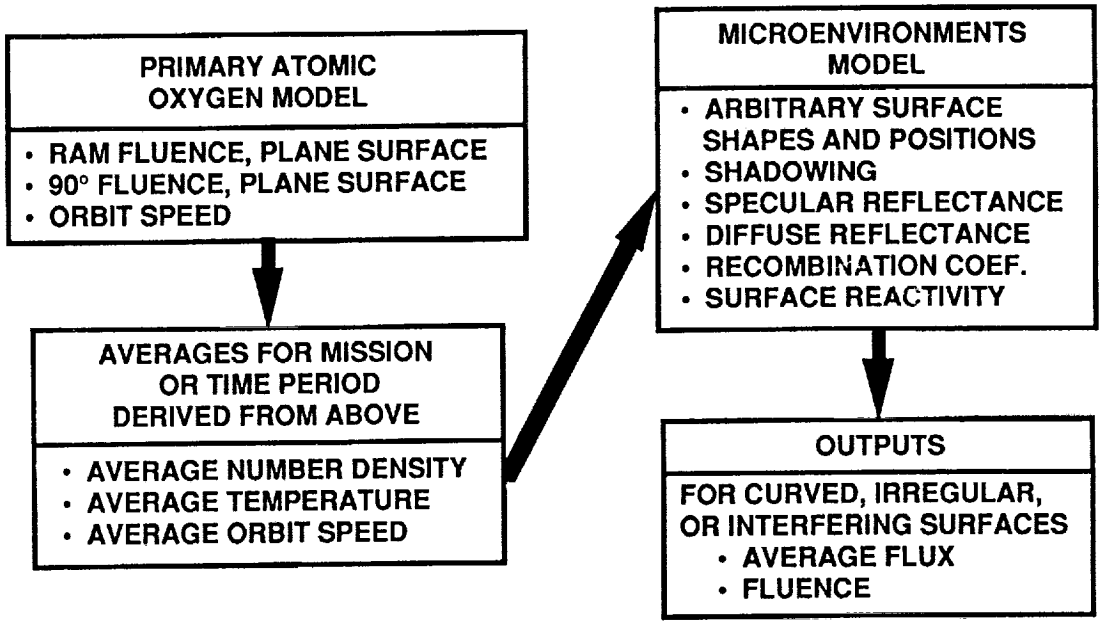

Figure 2. Attributes of the microenvironments model.

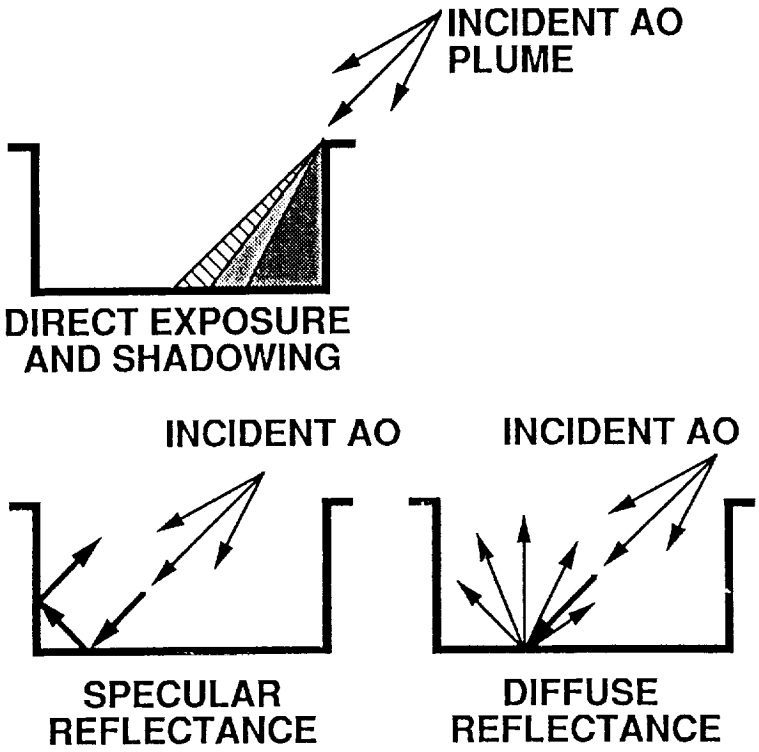

Figure 3. Shadowing, specular reflection and diffuse reflection of atomic oxygen on a spacecraft surface of complex shape.

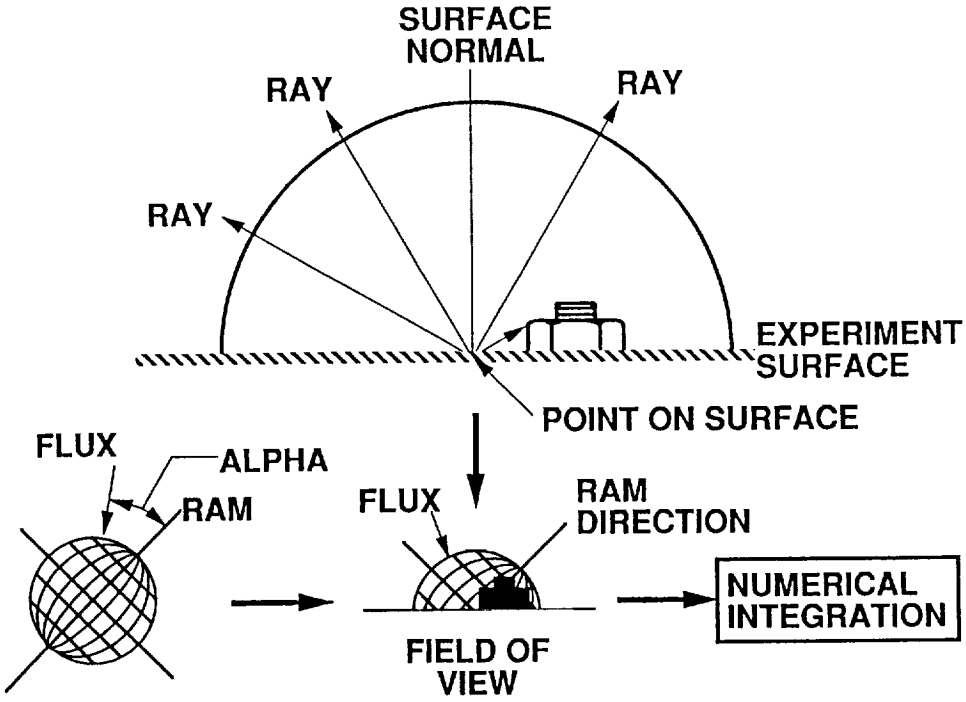

Figure 4. Four major elements of the microenvironments model; geometric routine, ray tracing routine, source function, and numerical integration routine.

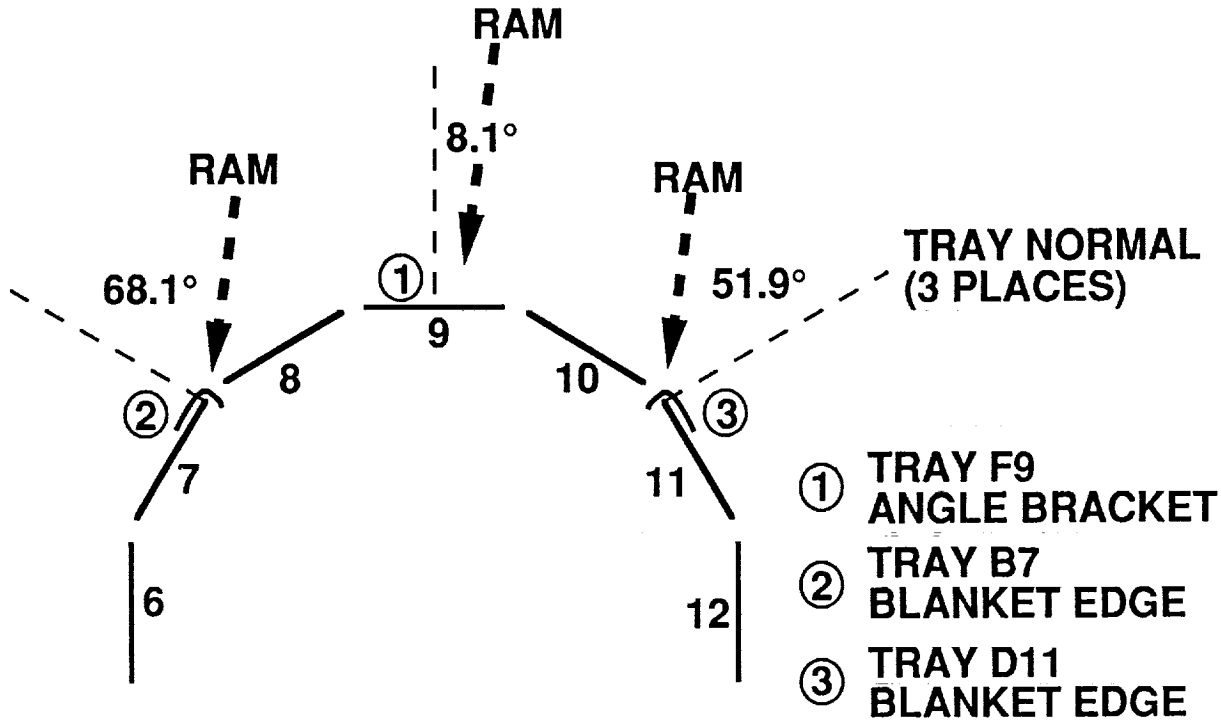

Figure 5. Location of FEP specimens used for experimental verification of the microenvironments model.

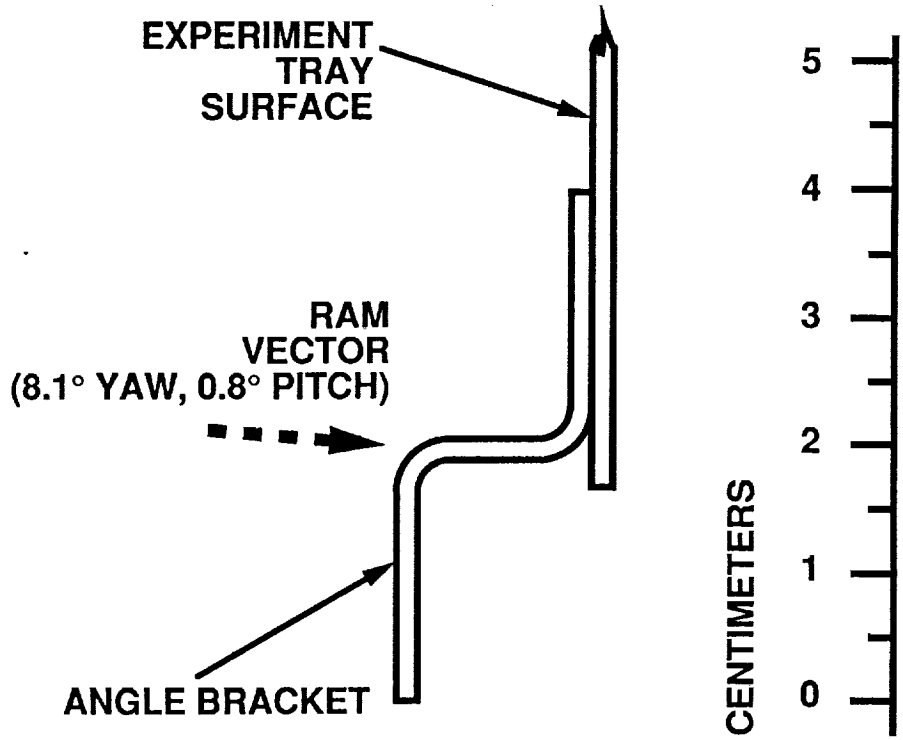

Figure 6. Shape of the angle bracket on Experiment Tray F9.

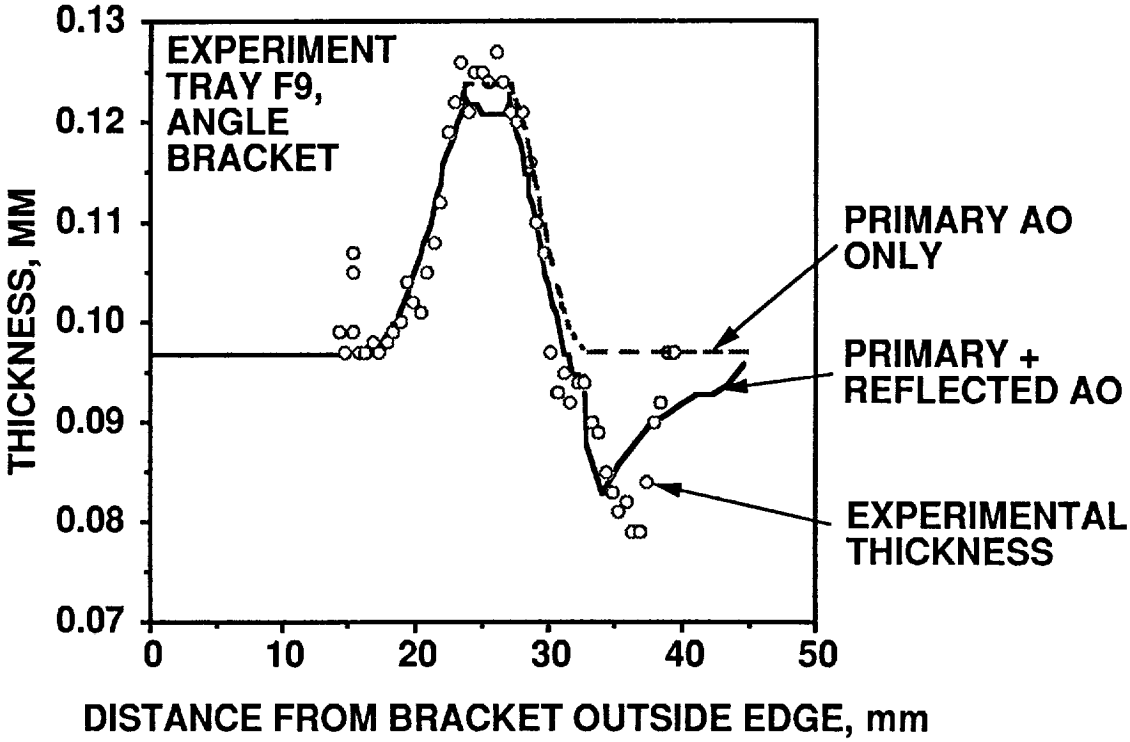

Figure 7. Comparison of observed and predicted erosion of the FEP film covering on the angle bracket.

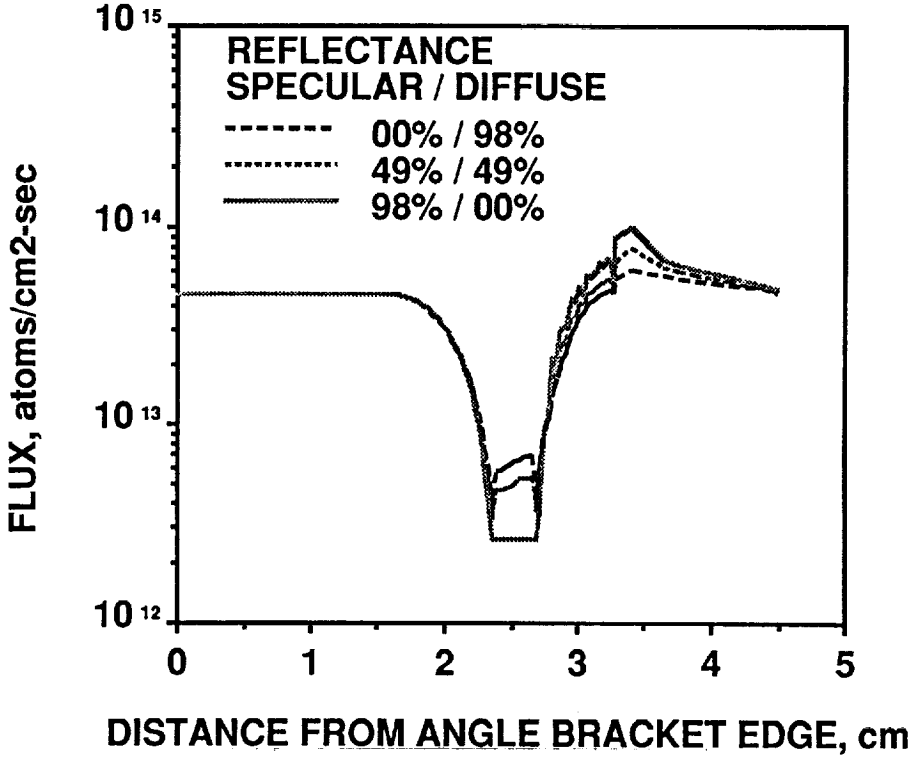

Figure 8. Effect on exposure of the angle bracket FEP film covering caused by varying molecular reflectance.

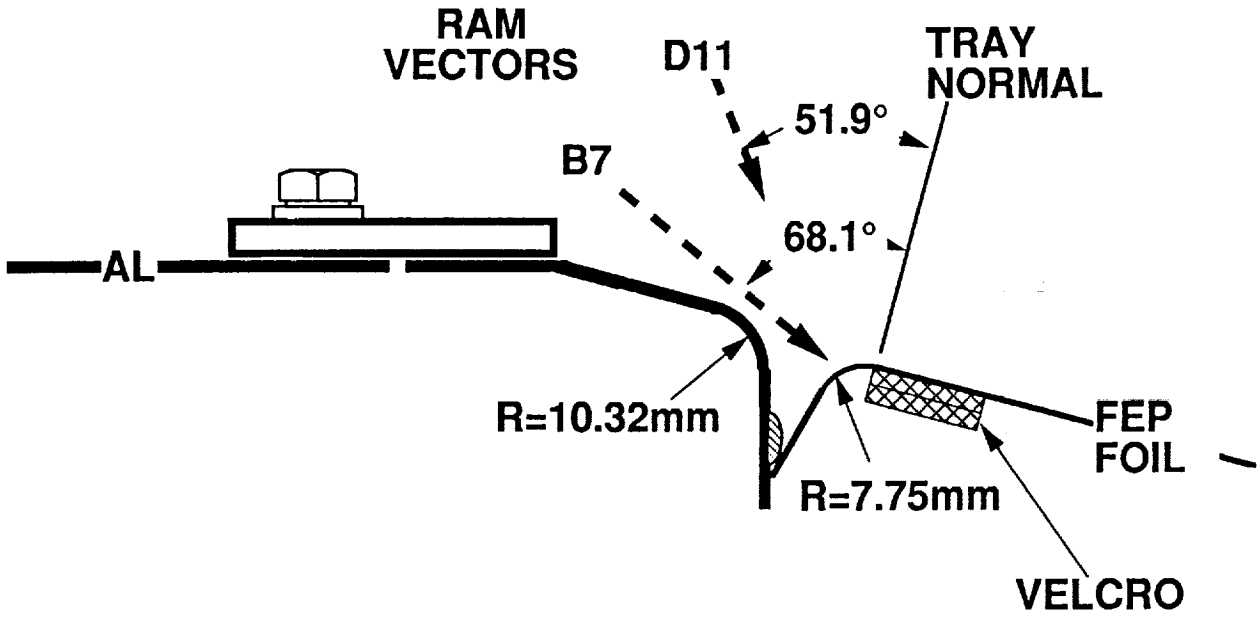

Figure 9. Shape of the edge attachment holding the thermal control blanket, Experiment Trays B7 and D11.

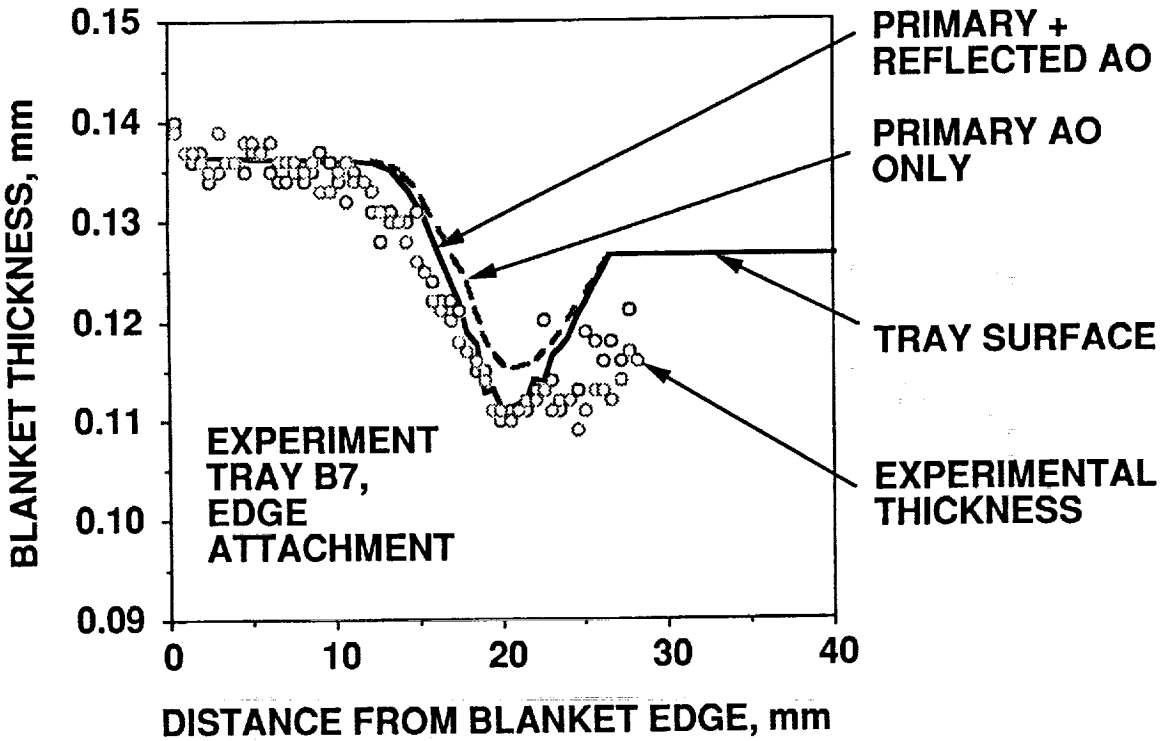

Figure 10. Comparison of observed and predicted erosion of the thermal control blanket at its edge attachment, Experiment Tray B7.

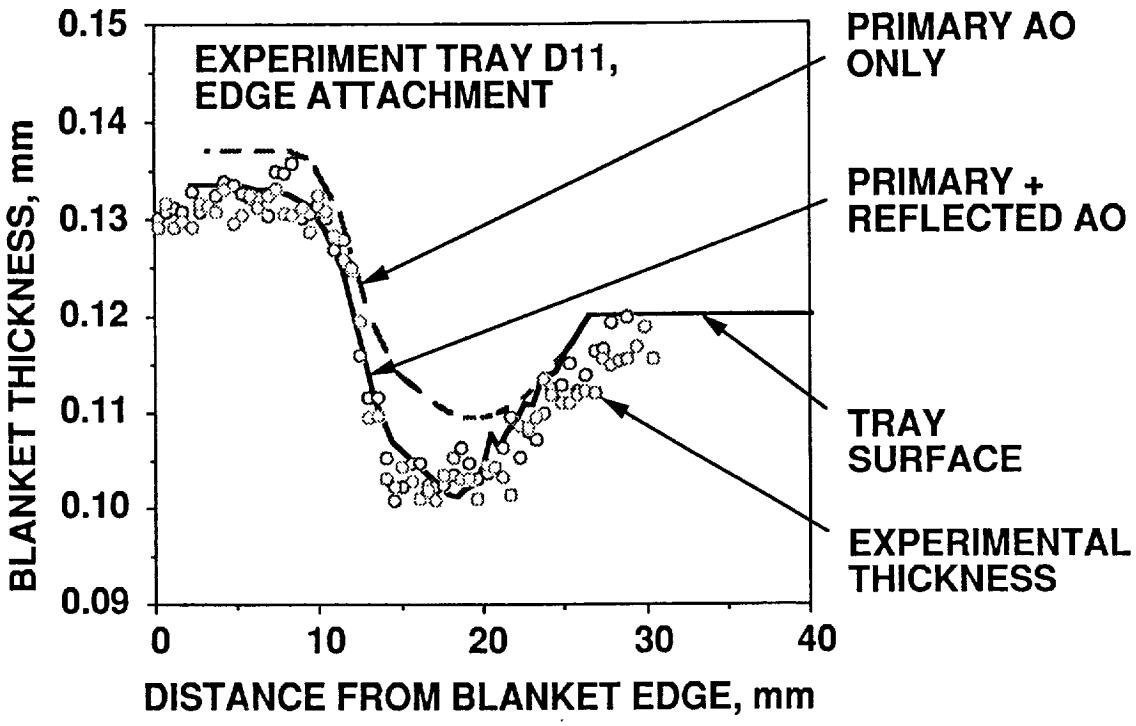

Figure 11. Comparison of observed and predicted erosion of the thermal control blanket at its edge attachment, Experiment Tray D11.